KfK 4506
Januar 1989

Sintered Glass

S. Gahlert, G. Ondracek
Institut für Material- und Festkörperforschung

Kernforschungszentrum Karlsruhe

Kernforschungszentrum Karlsruhe

Institut für Material- und Festkörperforschung

KfK 4506

Sintered Glass

S. Gahlert, G. Ondracek*

*jetzt: Institut für Gesteinshüttenkunde
Rheinisch-Westfälische Technische Hochschule
Aachen

Kernforschungszentrum Karlsruhe GmbH, Karlsruhe

CHAPTER 2

SINTERED GLASS

S. GAHLERT and G. ONDRACEK

Institut für Material- und Festkörperforschung, Kernforschungszentrum and Universität Karlsruhe
D-7500 Karlsruhe, Fed. Rep. Germany

Contents

Radioactive waste forms for the future, eds W. Lutze and R.C. Ewing

1. Introduction

In nuclear waste conditioning borosilicate glass has become the reference product in various countries. The term "borosilicate glass" usually implies a production via melting technology. For melting however, temperatures in the range of about 1400 to 1500 K are needed, giving rise to various problems, such as:

- Evaporation losses lead to changes in composition and produce secondary waste: volatility of radionuclides (e.g. Cs, Mo, Te and Ru) is much enhanced above 1100 K, whereas up to about 900 K volatility is dominated by decomposition of nitrates.
- Interactions occurring at elevated temperatures between the melt, crucible and melter material cause changes in the service life of equipment and also lead to variations of product compositions that are difficult to control.
- The liquid state, present at elevated temperature, allows segregations, as well as macroscopic inhomogeneities of the product. Also process control may become more complicated, e.g. in the LFCM (liquid fed ceramic melter) process, sedimentation of noble metals on the melter bottom may even disrupt power supply for direct heating.
- Cooling down from high temperatures leads to temperature gradients generating compressional stresses in the center and tensile stresses on the surface of the glass product; differences in thermal expansion of glass and stainless steel container cause compressional stresses on the glass surface (partially compensating the tensile stresses), and high tensile stresses in the container, facilitating stress corrosion in contact with water.

Since most of these problems are linked to the high temperature required for glass melting, in 1982 a program for the immobilization of high-level waste (HLW) via powder technology was initiated at KfK (Kernforschungszentrum Karlsruhe).

Sintering of high-level waste into a glass matrix was first tried by Ross (1975). He calcined the waste in a spray calciner at 770 K before mixing with glass frit. However, he observed a reaction between calcine and glass giving a potential for swelling. Such a reaction was not found by Terai et al. (1978), who investigated pressure sintering of simulated HLW with different glasses. Terai et al. reached good densities with Pyrex glass frit at 920 K. Chemical durability of their glass products was comparable to borosilicate glasses. In their experiments they used a pressure of 25 MPa. For the hot-pressing of glass however, pressures in the range of a few MPa are sufficient for good densification. Their work was also limited to laboratory-scale samples of 20 mm diameter; they did not examine the implications of increasing product dimensions. Macedo developed the Porous Glass Matrix process (PGM process) for the fixation of HLW in a high-silica glass matrix by sintering (Macedo et al. 1979, 1982). In the PGM process a borosilicate-type base glass is phase-separated by heat treatment. The low-silica phase is leached in HCl

and washed out. The remaining fine powder is soaked with HLW, dried under vacuum by gradual heating up to 1123 K, ground or ball-milled and finally sintered at 1473 K to a dense solid, consisting of a matrix of 96% SiO_2 and 4% B_2O_3 in which the waste elements are trapped. The main advantage of the process is the high chemical durability of the final product. The rather complicated process technology, also leading to the generation of secondary waste (e.g. washing solution), is considered a disadvantage.

Preliminary studies performed in the frame of CAB-KfK (Argentine-German cooperation between Centro Atomico Bariloche and Kernforschungszentrum Karlsruhe) showed that conventional sintering of dried glass-HLW mixtures (cold-pressing and subsequent sintering) would yield sufficient densities only for laboratory-scale diameters (≤ 20 mm) of the glass products (compare Bevilacqua et al. 1985). By hot-pressing (pressure sintering) however, highly dense glass products could also be prepared on a larger scale. The technology has now been developed for a product with a diameter of 30 cm. Corrosion problems, inherent in melting technology, are avoided by the in-can hot-pressing technique. In addition, the use of stackable containers, easily to arrange, may facilitate remote handling. Since hot-pressing temperatures for borosilicate glass are only in the range of about 900 to 1100 K, evaporation losses are reduced considerably. Process technology can be kept relatively simple by avoiding a separate calcination step. Product properties relevant to final storage or disposal are comparable to or better than properties of borosilicate glasses prepared by melting. In particular, because of the low hot-pressing temperatures, a more durable glass matrix with a higher silicon content and a lower sodium content, exhibiting better chemical durability, can be used. In hot-pressed simulated HLW-glass mixtures, most waste elements are *not* in solid solution in the glass, but rather heterogeneously embedded in the glass matrix, because the liquid state is avoided. Therefore, higher waste loadings can also be realized, since due to solid state densification segregation cannot take place and solubility limits of waste elements no longer impose restrictions.

2. *Waste loading*

In principle, waste composition should influence processing conditions and product performance only to a minor extent. In fact, HLW from reprocessed light water reactor fuel (LWR) and of fast breeder fuel (SBR), as well as dissolver sludge from LWR, was immobilized in borosilicate glass. However, only immobilization of LWR and SBR will be described in this chapter. Powder mixtures of LWR (SBR) waste simulant with VG98/12 (SG7) glass frit and the resulting hot-pressed products will be denoted by VG98/12-xLWR (SG7/xSBR), with x indicating the weight percentage of waste oxides.

Waste loading was varied between 5 and 35 wt%, even at 35 wt% final densities of more than 95% TD (theoretical density) could be reached. In this context 100% TD is understood as the density of a molten product. The insensitivity of product quality to variations in waste composition and waste loading simplifies process

Table 1
Composition of LWR and SBR waste simulate (HLLW concentration approximately 428 ℓ/tHM)

Element	LWR [a] [g/ℓ]	SBR [b] [g/ℓ]
Ba	4.96	2.85
Ce [e]	11.86	11.82
Cr	1.05	2.34
Cs	6.62	8.25
Fe	4.03	4.67
La	3.55	2.45
Mo [c]	13.18	8.28
Nd	11.51	7.06
Pd [d]	5.71	6.45
Pr	3.32	2.38
Rb	0.91	0.45
Ru	6.30	6.50
Sm	2.52	1.82
Sr	2.16	1.02
Te	1.67	1.22
Y	1.23	0.54
Zr	14.67	5.47

[a] Burnup approximately 40 GWd/tHM.
[b] Common reprocessing of inner core (burnup approximately 57.4 GWd/tHM) and axial blanket (burnup approximately 1.95 GWd/tHM).
[c] Mo also provides the Tc content.
[d] Pd also provides the Rh content.
[e] The actinides are simulated by Ce.

control and may even lead to cost reductions, if higher waste loadings might be favored (possibly after extended intermediate storage periods leading to considerable decrease in thermal activity). All samples were prepared using inactive waste simulant (table 1).

3. *Preparation of waste form and process technology*

3.1. Research line

The low temperature range, necessary for the preparation of hot-pressed HLW/glass, is one of the main important features. Careful investigation of preparation techniques was started on a laboratory-scale basis with samples up to 26 mm diameter. After establishing the main parameters for handling of the liquid waste, for mixing with glass frit, and for hot-pressing, an inactive demonstration line was set up for the production of full-sized samples with 30 cm diameter. A schematic overview of the process is given in fig. 1. In the following, first the characteristics

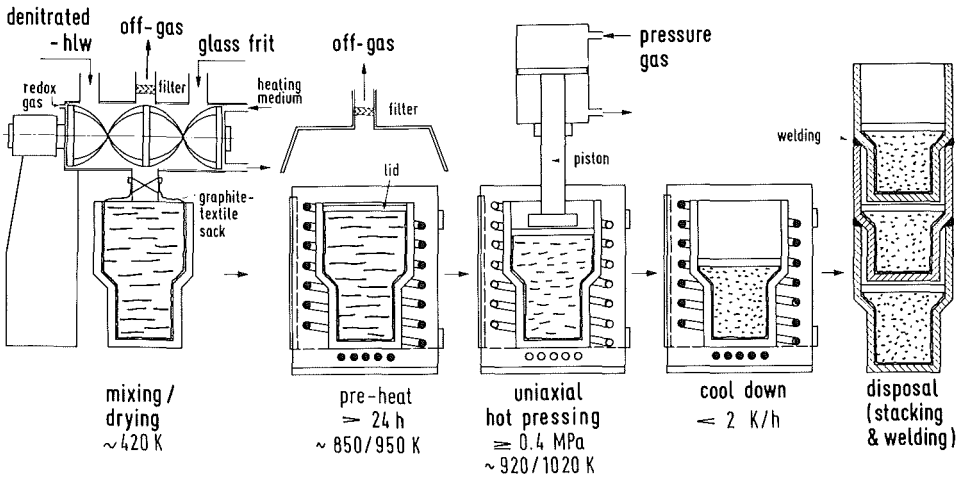

Fig. 1. Conditioning of radioactive waste by powder technology.

of the laboratory-scale preparation will be outlined. The demonstration line for full-sized sample production will be described in section 3.7.

3.2. General hot-pressing conditions

All laboratory-scale samples were prepared using an induction heated press, equipped with a programmable temperature controller based on a low-temperature pyrometer. In addition, temperatures were monitored by nickel-chromium-nickel thermocouples. Pressure was applied uniaxially, using a pneumatic system capable of producing low pressures in the range of 0.2 to 2 MPa. The samples were hot-pressed under helium atmosphere in graphite dies lined with graphite paper (to reduce friction). Density variations during hot-pressing were registered by a linear transducer monitoring the movement of the upper piston. Sample diameters were varied between 10 and 26 mm, with the standard sample having a diameter of 26 mm and a mass of 20 to 40 g.

3.3. Hot-pressing of glass frit

The sintering of glass is governed by viscous flow (Frenkel 1945, Kuczynski 1949, Kingery and Berg 1955). Glass frit (crushed glass) however, may deviate from the Frenkel sintering equation for spherical glass particles:

$$\Delta L/L_0 = \gamma t/2\alpha\eta, \tag{3.3.1}$$

where

$\Delta L/L_0 = (L_0 - L)/L_0$,

L = length of compact at time t [m],

L_0 = original length of compact [m],

γ = surface tension [N/m],

α = average radius of the spherical particles [m],

η = viscosity of glass [Pa s].

For example, Cutler and Henrichsen (1968) showed, that crushed glass sinters much more rapidly than spherical glass particles. In addition, the loss of water can effect sintering behavior considerably [for a good review on gases and water in glass see Scholze (1966)].

In fig. 2 the results of the thermal gravimetric analysis (TGA) of the two glass frits used in the hot-pressing experiments, VG98/12 and SG7, are depicted. VG98/12 is a borosilicate glass developed at KfK for the melting process LFCM (Guber et al. 1979). SG7 was developed specially for the hot-pressing of HLW with glass frit. It contains more silicon and aluminum, and less sodium than VG98/12 (cf. table 2).

The slow loss of weight of glass on heating above 400 K is typical of the driving off of chemisorped material, in this case water from the condensation reaction:

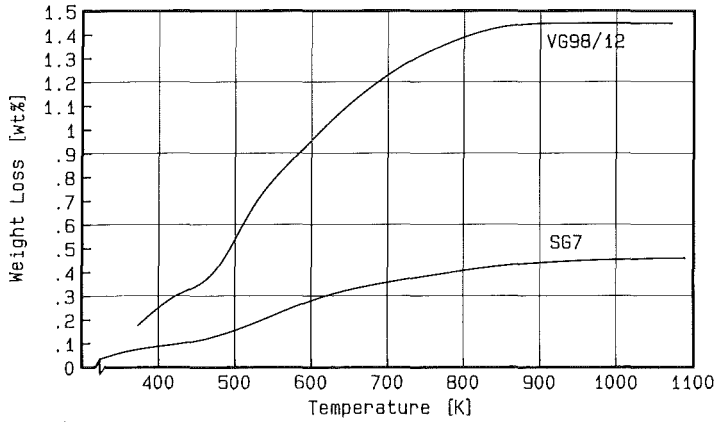

Fig. 2. TGA of glass frits VG98/12 and SG7; heating rate 1 K/min; sample mass 1753 mg (VG98/12) and 2656 mg (SG7).

Table 2
Powder characteristics of glass frits VG98/12 and SG7

Chemical composition [wt%]		VG98/12	SG7
Al_2O_3		2.6	8.6
B_2O_3		12.4	8.3
CaO		4.1	2.7
MgO		2.1	1.0
Na_2O		17.5	7.4
SiO_2		56.7	72.0
TiO_2		4.6	–
Transition temperature [K]		810	840
Density [kg/m^3]		2554	2375
Particle size	<1 μm	9.9	7.7
Distribution [wt%]	<6 μm	47.8	42.6
	<32 μm	99.0	93.5
Median particle size [μm]		5.5	7.7

$2SiOH \rightarrow Si—O—Si + H_2O$. Water analyses showed that weight loss corresponds closely to the loss of water. The compositions and other characteristic data of VG98/12 and SG7 are given in table 2, their particle size distributions are plotted in figs. 3a and 3b. The particles have an edged surface geometry typical for fragments resulting from the crushing of glass.

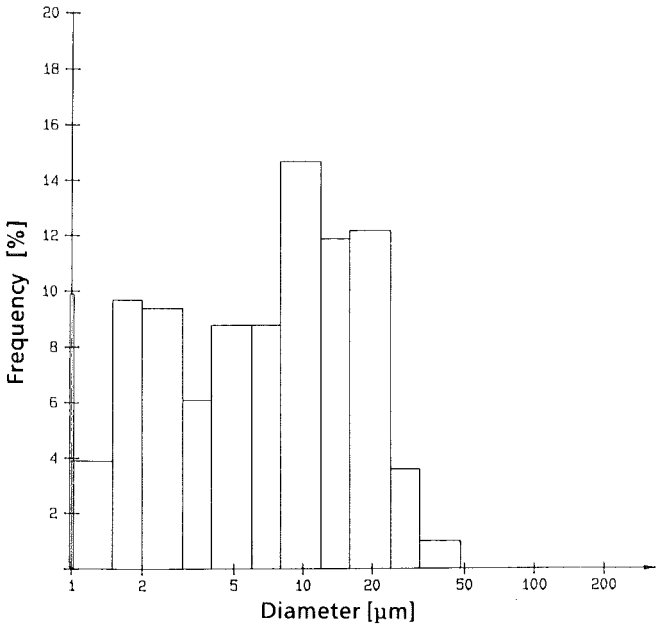

Fig. 3a. Particle size distribution of glass frit VG98/12.

The lower sodium content of SG7, as well as the smaller median particle size of VG98/12 may explain the higher weight loss of the latter. During hot-pressing operation no loss of water or gases should occur to avoid swelling of the product. Hot-pressing temperatures of VG98/12 (SG7) are in the range of 870 to 920 K (970 to 1020 K). When comparing the weight loss characteristics of the glass frits to their hot-pressing temperature, the glass, especially VG98/12, may still lose water during hot-pressing. With high heating rates, sintering will begin on the surface, leading to a dense outer shell, while in the interior temperatures are lower. Therefore in this temperature range the loss of water will lead to a potential for blistering or swelling. In this context SG7 exhibits a more favorable behavior, since the total generation of water is only about a third of that of VG98/12. However, both glass frits can be hot-pressed to high densities, if heating rates are controlled carefully. In figs. 4a and 4b, the final densities reached by hot-pressing of VG98/12 and SG7 are shown.

Temperature is clearly the most important variable in hot-pressing of the given glasses. For VG98/12 the optimum temperature is ~890 K, a temperature rise by 60 K leads to a decrease in final density of ~6%. This behavior, not common in

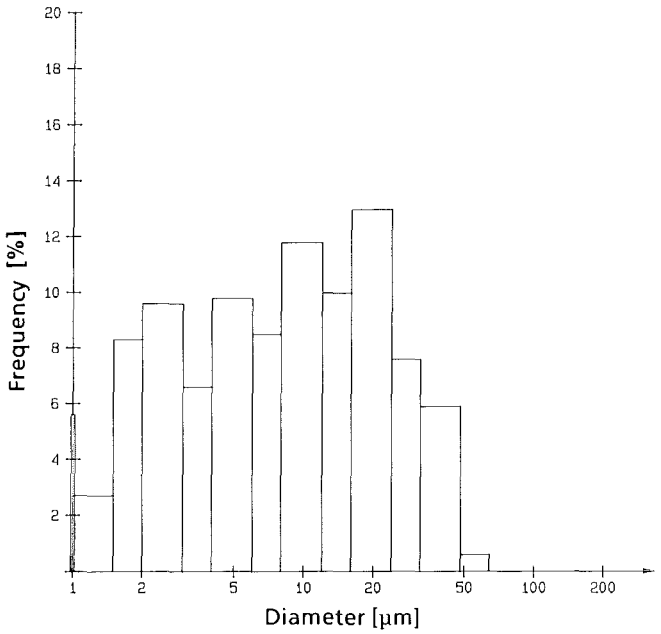

Fig. 3b. Particle size distribution of glass frit SG7.

glass sintering, can be explained by internal gas pressure, resulting from residual water. The optimum temperature for hot-pressing of SG7 is about 1020 K. Although SG7 behaves similarly to VG98/12, the effect of raising the temperature above the optimum value is much less pronounced (a temperature increase of 60 K leads only to a density decrease of less than 1%). The samples were hot-pressed according to the following program:

- heating to 850 K (VG98/12) or 950 K (SG7); heating rate 100 K/min;
- degassing for 15 min at 850 K (VG98/12) or 950 K (SG7);
- heating to the desired hot-pressing temperature (893, 923 or 953 K for VG98/12; 993, 1023 or 1053 K for SG7); heating rate 5 K/min;
- applying pressure (0.4 to 1.0 MPa); hot-pressing till no further densification occurs (about 10 to 15 min);
- cooling to room temperature; cooling rate ~5 K/min.

Especially in hot-pressing of VG98/12, the degassing step is important for the release of residual water. If this step is deleted or shortened considerably, the samples will contain blisters. Also increasing heating rates above the given values will lead to lower final densities.

3.4. Characteristics of simulated HLW

The thermal stability of the waste simulants was investigated by thermogravimetric analysis (TGA). Figure 5 shows the evaporation loss of LWR (SBR) waste simulant after drying at 420 K.

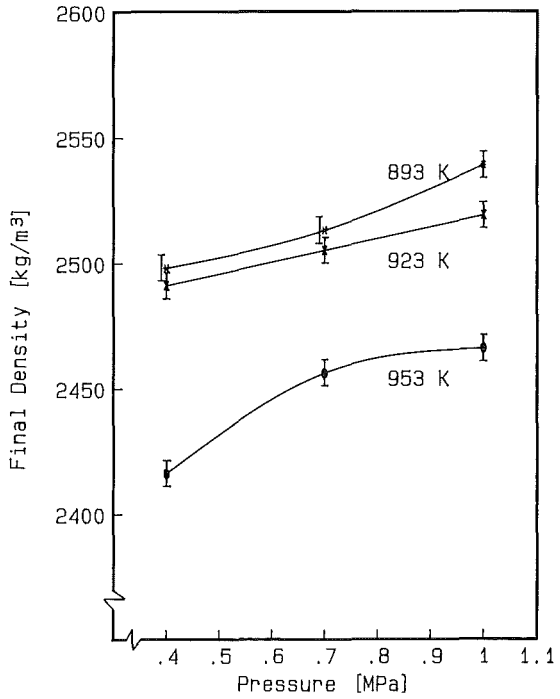

Fig. 4a. Influence of hot-pressing temperature and pressure on final density of VG98/12 (diameter 26 mm).

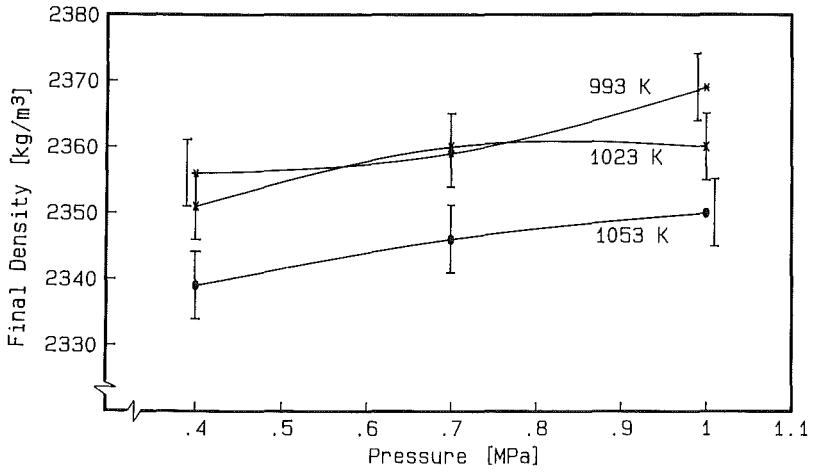

Fig. 4b. Influence of hot-pressing temperature and pressure on final density of SG7 (diameter 26 mm).

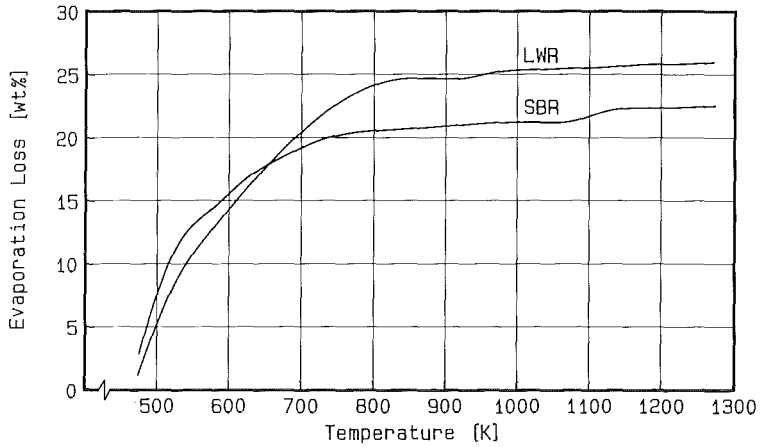

Fig. 5. TGA of denitrated LWR waste simulant (sample mass 260 mg) and SBR waste simulant (373 mg sample mass) after drying at 420 K, heating rate 1 K/min.

In Table 3 the residual nitrate and nitrite content of LWR waste simulant, determined by chemical analysis of LWR, calcined at different temperatures for 24 h, is given. The comparison with the evaporation loss (fig. 5) shows that up to 900 K the off-gas is clearly dominated by the decomposition of nitrates. This is consistent with the results by Bauer and Ondracek (1983). If the waste is not calcined before mixing with glass frit, sintering is possible only in a temperature range, where no further weight loss occurs during the sintering process, i.e. 850 to 930 K (LWR) or 950 to 1070 K (SBR). Thus LWR can be hot-pressed with VG98/12 in the desired temperature range, whereas for SBR waste a glass frit with a higher hot-pressing temperature would be desirable. Therefore the new glass SG7 was developed for the immobilization of SBR waste.

3.5. Preparation of simulated HLW/glass mixtures

The high-level liquid waste (HLLW) was prepared by dissolving the oxides or nitrates, in water and nitric acid. The resulting ~5 molar nitric acid solution was

Table 3
Residual nitrate and nitrite content of calcined LWR and SBR waste simulate (calcination time >24 h)

Calcination temperature [K]	Nitrate content [wt% NO_3]	Nitrite content [wt% NO_2]
423	23.00	1.20
573	5.00	<0.01
673	1.60	<0.01
773	0.17	<0.01
873	<0.01	<0.01
973	<0.01	<0.01
1073	<0.01	<0.01

denitrated with ~40 vol% of formaldehyde. During denitration most waste elements precipitate from the solution and pH rises to ~3.5. If the noble metals (Ru, Rh and Pd) are deleted from the waste simulant, the reaction is not as brisk and final pH is only ~1.5. Obviously the noble metals have some kind of catalytic effect on denitration. After denitration the residues were mixed with glass frit, dried in a flask and subsequently calcined in a separate furnace at 820 K (VG98/12) or 920 K (SG7), respectively. (These temperatures represent the highest values possible, before the mixtures show clear signs of sintering.) Before hot-pressing, the calcine was ground in a vibration mill for 15 s to destroy any agglomerates caused by drying and calcining. The resulting powder comprised an intimate mixture of glass and HLW simulant.

3.6. Hot-pressing of simulated HLW/glass mixtures

The HLW/glass mixtures were hot-pressed according to the same temperature program as given in section 3.3. The resulting final densities of VG98/12-15LWR and SG7-15SBR products are shown in figs. 6a and 6b. Clearly, for VG98/12-15LWR, there is an optimum temperature, ~920 K, for hot-pressing. Raising the hot-pressing temperature by 30 K leads to a sharp decrease in density, if pressure is kept below 1 MPa. This behavior can be easily explained by the evaporation

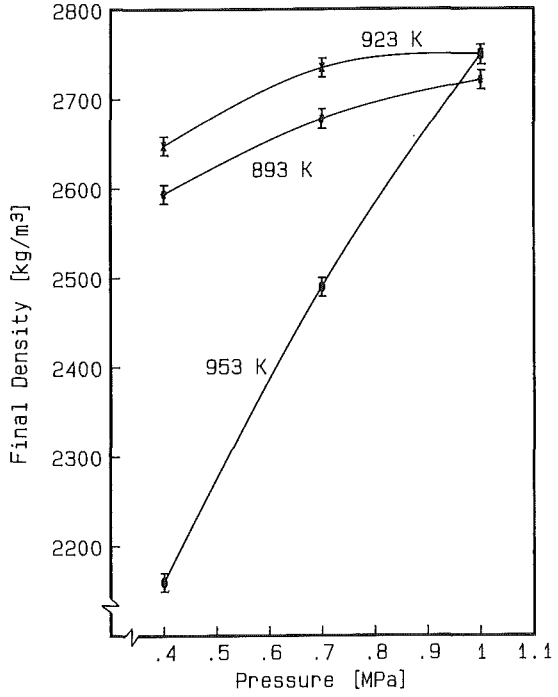

Fig. 6a. Influence of hot-pressing temperature and pressure on final density of VG98/12 containing 15 wt% of simulated LWR waste oxides (26 mm diameter).

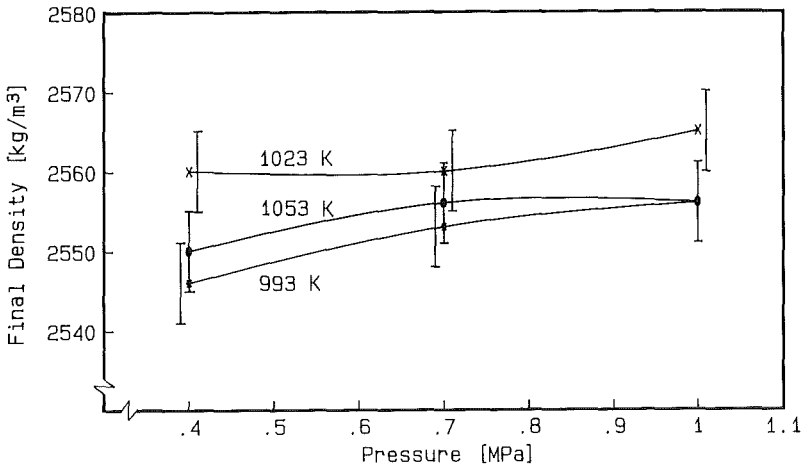

Fig. 6b. Influence of hot-pressing temperature and pressure on final density of SG7 containing 15 wt% of simulated SBR waste oxides (26 mm diameter).

characteristic of LWR (fig. 5). Only between 850 and 930 K weight is constant. Above 930 K, evaporation loss begins to rise again. Obviously the resulting internal gas pressure can be overcompensated by higher pressures, leading to dense final products. These products however, will show a tendency towards swelling, if heated above the glass transition temperature (810 K). Consequently, hot-pressing temperatures should not exceed 930 K.

The optimum hot-pressing temperature for SG7-15SBR is ~1020 K. Higher temperatures however, lead only to small decreases in density. Again, this can be explained by the evaporation characteristic of the HLW (cf. fig. 5 for SBR simulate).

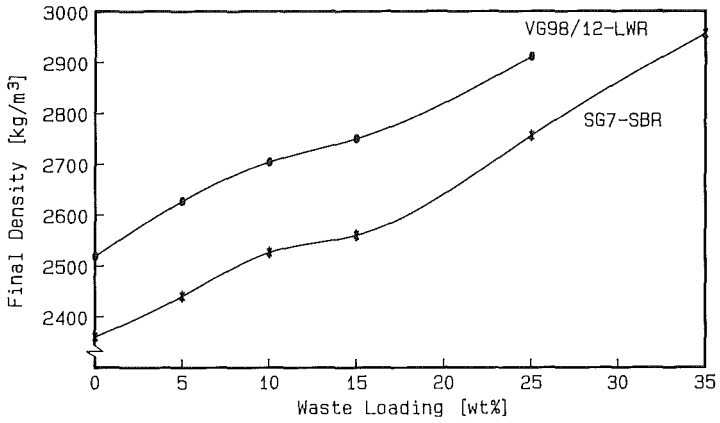

Fig. 7. Influence of waste loading on final density of hot-pressed VG98/12 with LWR waste simulate (1 MPa, 923 K) and SG7 with SBR waste simulate (1 MPa, 1023 K) (diameter 26 mm).

The influence of waste loading on final densities of VG98/12-LWR and SG7-SBR products is depicted in fig. 7. The samples containing up to 10 wt% of waste oxides have a very low porosity ($\leq 1\%$, measured by quantitative image analysis). At higher waste loadings porosities are slightly higher, as indicated by the changing slopes of both curves in fig. 7. Several effects may influence this behavior: one may be the Hedvall effect (cf. Meyer 1968, Thümmler 1963), which means that phase transformations or reactions occurring during the sintering process enhance sintering ability. At higher waste loadings however, this positive effect may be overcome by increasing internal gas pressure.

3.7. Inactive demonstration line for full-sized sample production

3.7.1. Research basis

The basic sintering studies described above, led to the conclusion that the in-can hot-pressing technique should provide a good possibility for the conditioning of HLW, also in a full-scale process. Therefore an inactive demonstration line was built.

3.7.2. Drying and mixing

A schematic diagram of the process is given in fig. 1. The equipment used for the production of full-sized samples is shown in fig. 8. The glass frit is fed together with the denitrated HLW simulate into a heatable mixer. The mixer is heated by oil, maintained at the desired temperature (420 K). To eliminate contamination, and to speed up drying, the mixer is held under low pressure (~0.08 MPa), produced by a water jet pump operating in a closed circle. For careful control of redox state additional air is fed to the mixture at a rate of 200 ℓ/h. A simple filter device was developed in order to retain solid aerosol particles from the off-gas. A box containing glass beads of the same composition as the glass frit to be processed, provides a filtration of the majority of the solids, accomplished by sieve and adsorption effects. If necessary, the glass beads may be exchanged by simply feeding into the mixer, to be processed with the next charge, avoiding the formation of secondary waste. The filter device is followed by a condenser and wash columns filled with dilute nitric acid and water, respectively. This arrangement limited the contamination of the wash columns by HLW simulant to a few ppm. The mixture is dried batch-wise (maximum 32 kg) during continuous blending for about 16 h. The resulting dry powder is fine (cf. figs. 9a and 9b for particle size distribution of VG98/12-15LWR and SG7-15SBR mixtures) and can be hot-pressed like the laboratory-scale mixtures that went through an additional grinding step.

3.7.3. Calcination and hot-pressing

After drying and mixing, the HLW-glass mixture is fed by gravity into stainless steel containers shaped for subsequent stacking (cf. fig. 1). The containers are lined with a graphite fabric sack that can be mounted directly to the mixer outlet, avoiding contamination during filling of the container. The graphite lining also reduces wall friction and compensates for differences in thermal expansion between the glass

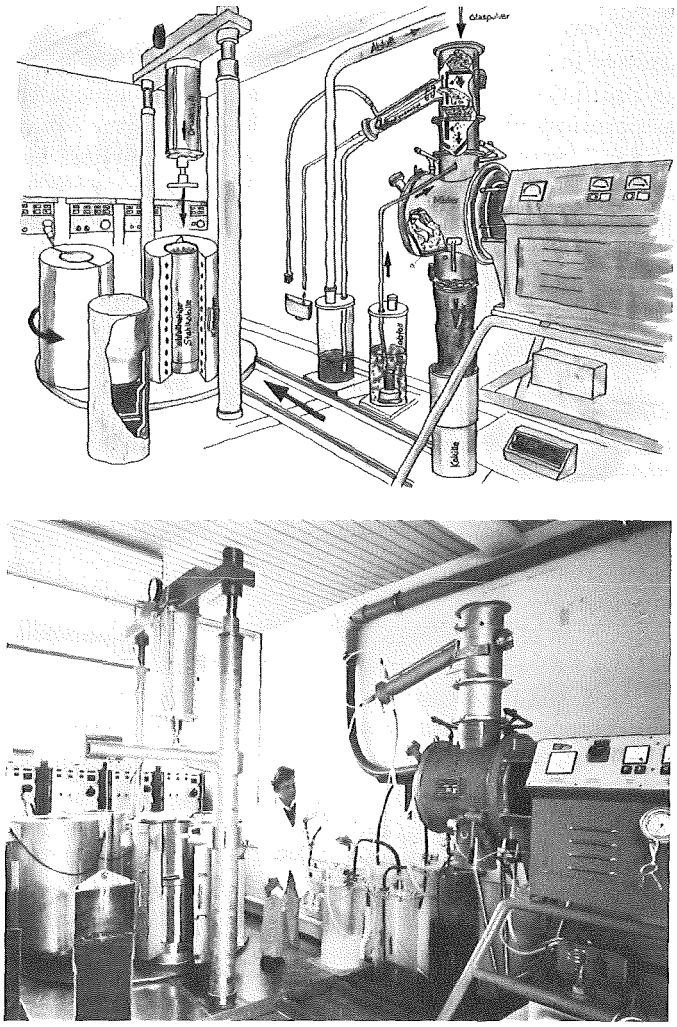

Fig. 8. Inactive demonstration line for full-sized sample production (scheme: top, reality: bottom).

product and steel. Afterwards, the containers are transferred to conventional electrical furnaces for in-can calcination and hot-pressing according to the following program:

- heating to 850 K (VG98/12) or 950 K (SG7) under air; heating rate 5 K/min;
- calcination for >24 h at 850 K (VG98/12) or 950 K (SG7);
- heating to 920 K (VG98/12) or 1020 K (SG7); heating rate 1 K/min;
- applying pressure (~0.4 to 1.0 MPa); hot-pressing till no further densification occurs (~4 to 6 h);
- slow cooling to room temperature to avoid cracking (<2 K/h).

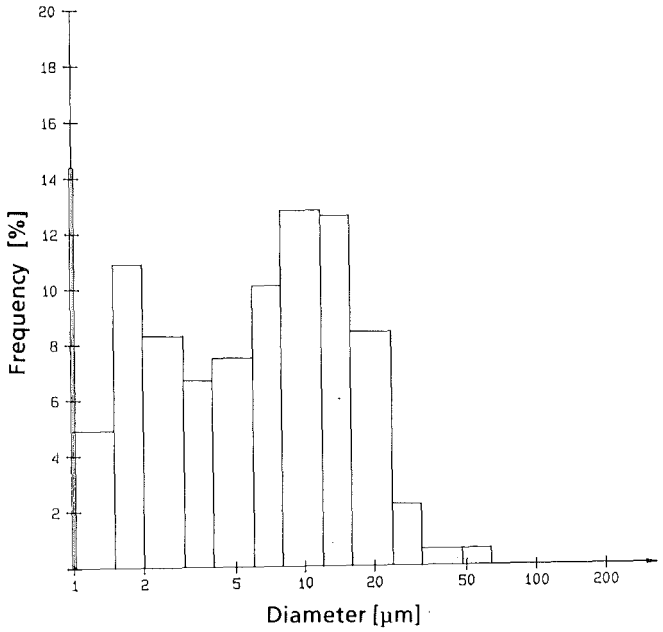

Fig. 9a. Particle size distribution of VG98/12-15LWR mixed for ~16 h.

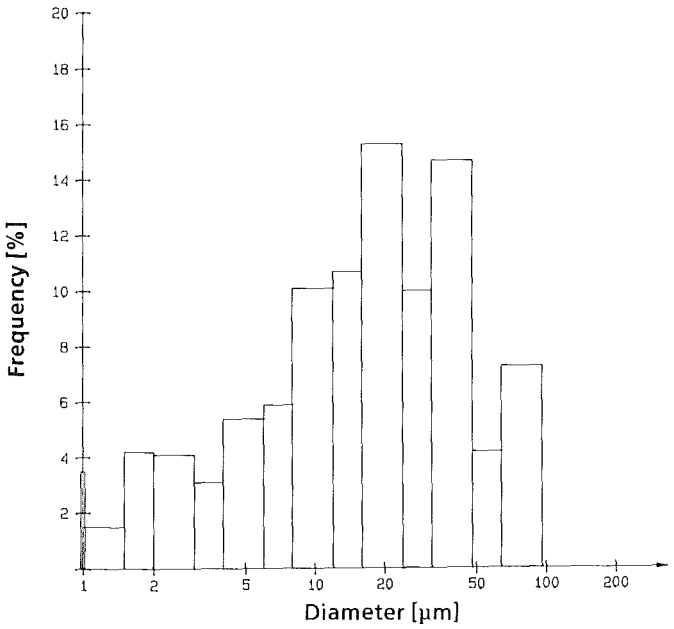

Fig. 9b. Particle size distribution of SG7-15SBR mixed for ~16 h.

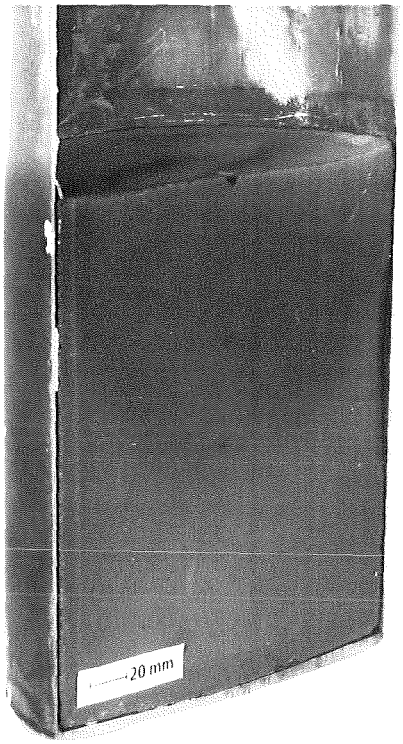

Fig. 10. Glass product VG98/12 containing 15 wt% of LWR waste simulate (19 cm diameter).

This temperature program corresponds closely to the program for hot-pressing of small, laboratory-scale samples. Of course, calcination, hot-pressing, and cooling times have to be adjusted to the larger diameters, i.e. larger volumes. This "in-can calcination" requires quite a long time when compared with a conventional, separate HLW calcination step; however "in-can calcination" simplifies the process to a great extent. A simple air-pressure device was used to generate the small pressure required for densification. Pressures higher than 1 MPa, lead to shorter sintering times, but are not necessary in order to reach high final densities. Since the hot-pressing step itself is quite short in comparison to the other times involved, only shorter calcination and cooling times would speed up the process as a whole. Therefore, parallel processing of 4 containers was chosen. While one container is preheated, the next is hot-pressed, and the other two are cooled at the same time. In addition, with self heating, active waste, cooling times, required to avoid or reduce cracking, will be shortened substantially, since final temperatures on the surface will be much higher than room temperature (400 to 600 K).

The glass products, produced as described above, were highly dense and crack-free (fig. 10). By X-ray fluorescence analysis on samples taken from different locations of the same product, it was shown that waste elements were distributed homogeneously on a macroscopic scale.

4. *Structure*

4.1. Distribution of elements and components

As mentioned earlier, hot-pressing of HLW-glass mixtures does not lead to solid solutions of waste oxides in glass as is common for borosilicate glasses made via

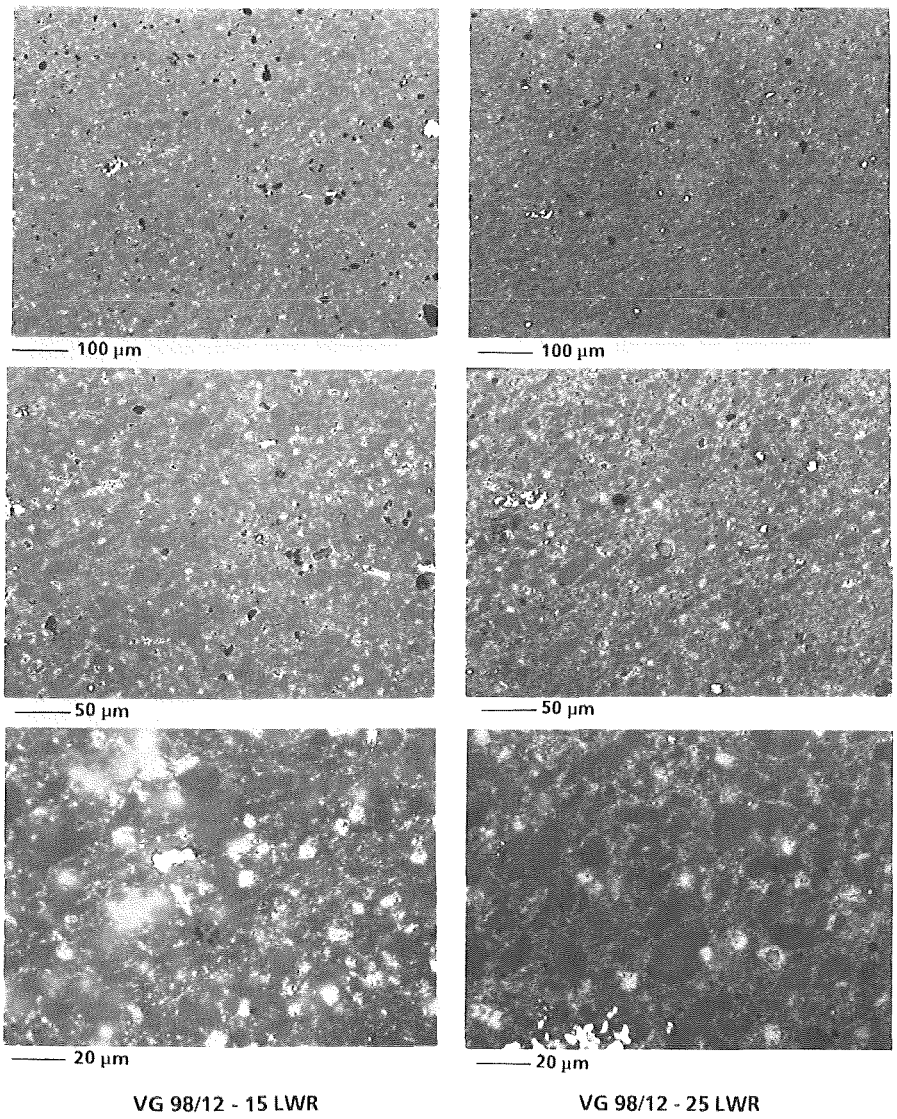

Fig. 11. Micrographs of VG98/12 glass products containing 15 and 25 wt% of LWR waste simulate (26 mm diameter).

melting. Most waste elements are rather encapsulated between glass particles, yet some elements (e.g. cesium) will diffuse into the glass matrix or react with other components, even at the modest hot-pressing temperatures. Figure 11 shows light optical micrographs of VG98/12 glass products, containing 15 and 25 wt% of LWR waste simulate, giving different magnifications of the same sections. The dark spots, visible at the lowest magnification (top), represent pores, while the brightest particles are noble metals (Ru, Rh, or Pd). At higher magnifications the pores cannot be seen as clearly because of the glassy matrix (at the highest magnification, bottom, pores appear as larger white, shining areas). The small white spots reflect mainly waste components that are arranged almost like a network around the larger grey areas representing nearly pure glass particles. The largest glass particles have a diameter of 20 to 30 μm, this corresponding to the original particle size (cf. fig. 3a).

The results of a microprobe analysis on VG98/12-15LWR are given in fig. 12. Clearly, barium, iron, neodymium, and cerium are distributed like a network around the larger glass particles, while cesium has diffused evenly into the glass matrix. Ruthenium (also rhodium and palladium not shown here) appear localized in the metallic state. The main glass constituents, silicon, sodium, aluminum, calcium, and oxygen are distributed more homogeneously. Obviously, some elements react to form new phases, as was detected by EDAX analysis. Ce, Nd, and Zr were found together with some Ca and Fe.

The structure of SG7 containing SBR waste simulant (fig. 13) is similar to the VG98/12 products. Optical micrographs are shown of SG7 glass products with SBR waste loading which varies between 5 and 35 wt%. The different magnifications are taken from the same sections.

The micrographs of samples containing higher waste loadings exhibit better contrasts due to increased absorbency of diffusive light, but their structure is generally the same. Again, the brightest spots represent noble metal inclusions, while most of the waste components (light grey) are arranged like a network around the darker glass particles. The average size of the glass particles is a little larger when compared to the VG98/12 products (diameters up to about 40 μm, cf. original particle size, fig. 3b). The distributions of some important elements, determined by electron microprobe analysis, are shown in fig. 14. These results are also similar to those obtained earlier with VG98/12 glass products. However, the VG98/12 products are generally hot-pressed at lower temperatures than SG7 glass products (920 K instead of 1020 K). This may explain the differences that can be observed:

- Cesium is dispersed completely homogeneously.
- Barium has diffused into the matrix, but has also formed some agglomerates.
- Calcium, as an original glass component is more homogeneously distributed and has reacted with some waste elements (e.g. Nd and Ce).

Higher temperatures facilitate a more homogeneous distribution of some elements because of their enhanced mobility. For some other elements, the possibility of new phase formations is increased at the same time. To investigate the effect of heat treatment on microstructure, SG7 and VG98/12 samples were annealed at 770 K. After 28 d microprobe analysis did not reveal any changes in elemental distributions. Some of the samples described above exhibit slight textures of the glass particles. However, this effect was never observed on full-sized samples. By contrast, the

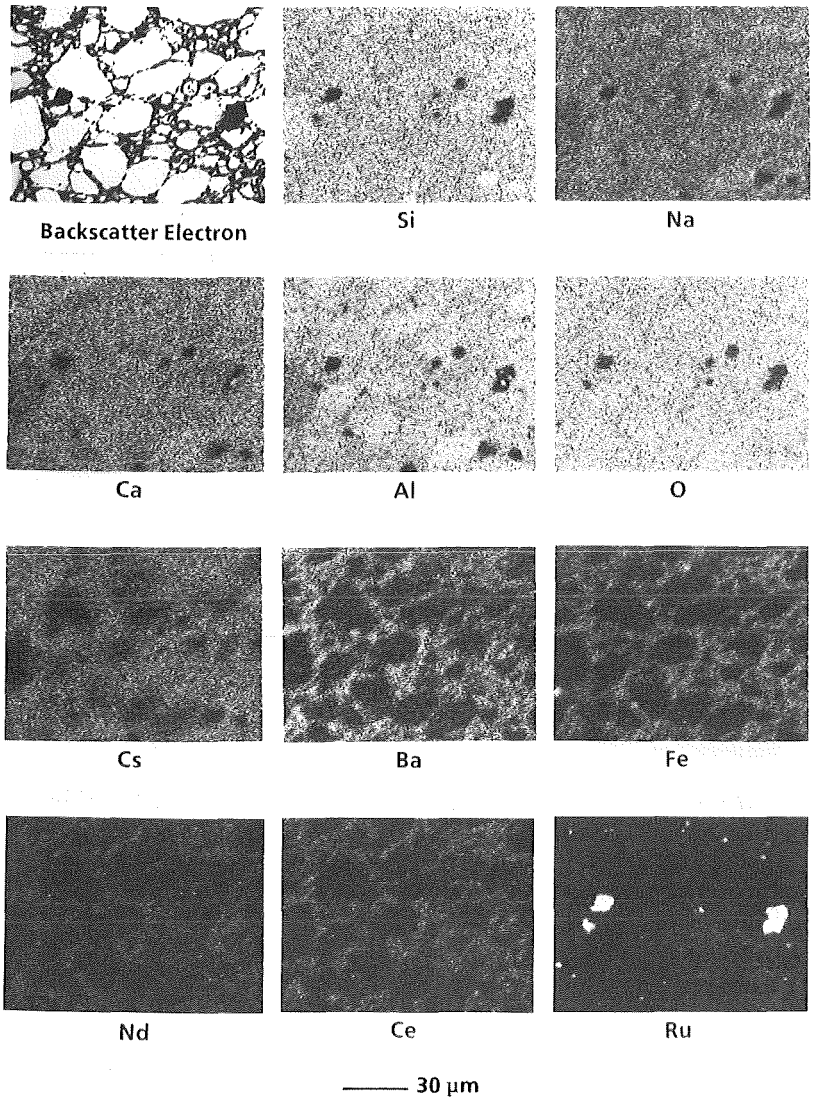

Fig. 12. Elemental distribution plots of VG98/12-15LWR glass product (26 mm diameter) by electron microprobe.

homogeneity of these products depends mainly on the quality of the mixture processed in the heatable mixer. As an example, fig. 15 shows the microstructure of VG98/12 and SG7 glass products (19 cm diameter). While the VG98/12 mixture with LWR waste simulate is homogeneous (left), the mixture of SG7 with SBR waste simulate (right) shows a special arrangement of the waste particles. The mixture was not wet enough at the beginning of the mixing step (liquid waste simulate was added only partially at the beginning), therefore agglomerates occurred. Mixing experiments demonstrated that wet mixing gives the most homogeneous mixtures. Agglomerates can be avoided by adding all of the liquid initially.

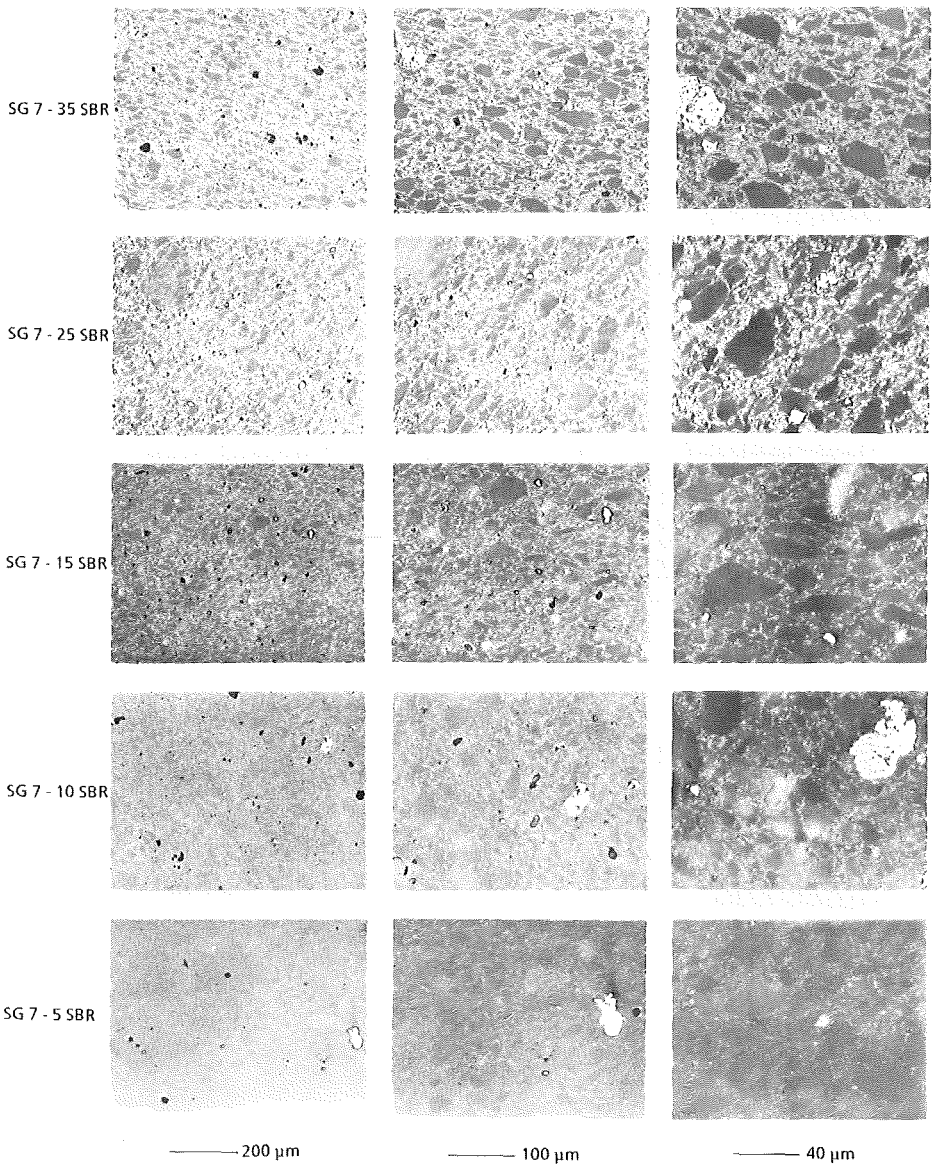

Fig. 13. Micrographs of SG7 glass products containing 5 up to 35 wt% of SBR waste simulate (26 mm diameter).

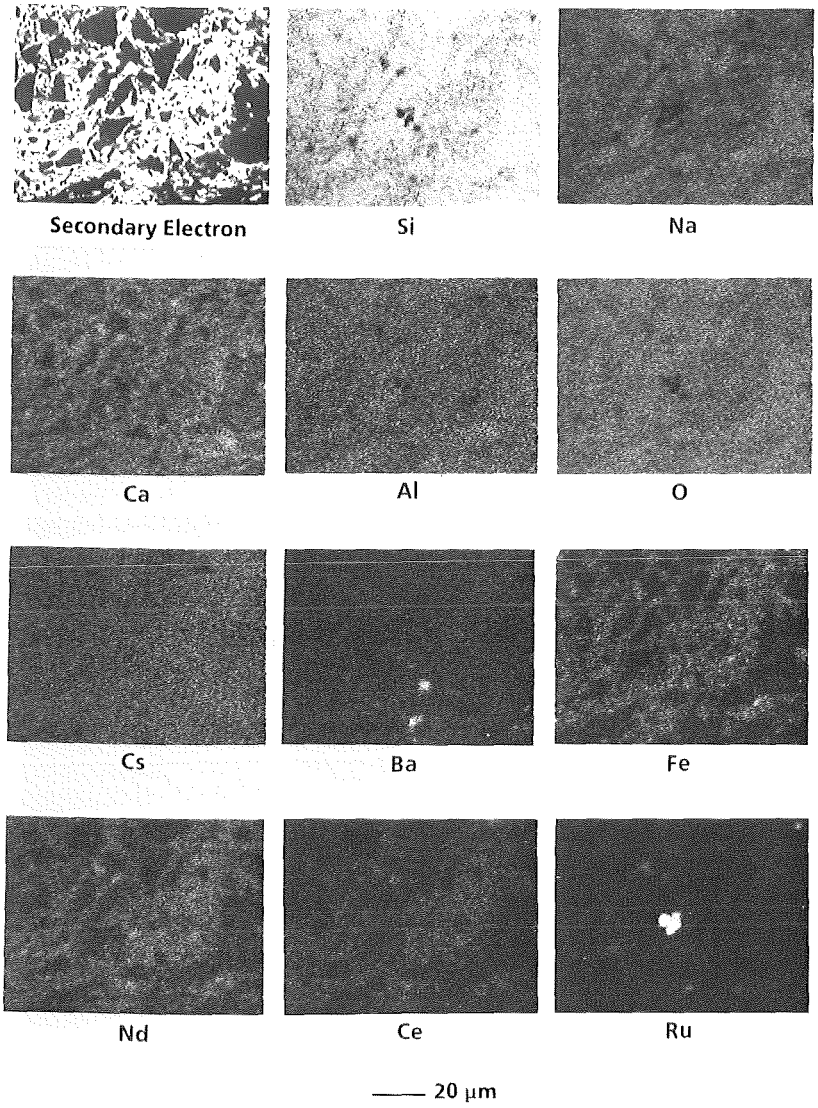

Fig. 14. Elemental distribution plots of SG7-15SBR glass product (26 mm diameter) by electron microprobe.

4.2. Devitrification

Crystallization of molten VG98/12 glass products containing simulated LWR waste oxides has been examined in detail by Skokan and Schauer (1982). After heat treatments up to 10 000 h at temperatures between 620 and 1020 K, they observed mainly two phases in addition to RuO_2 and Pd alloys:

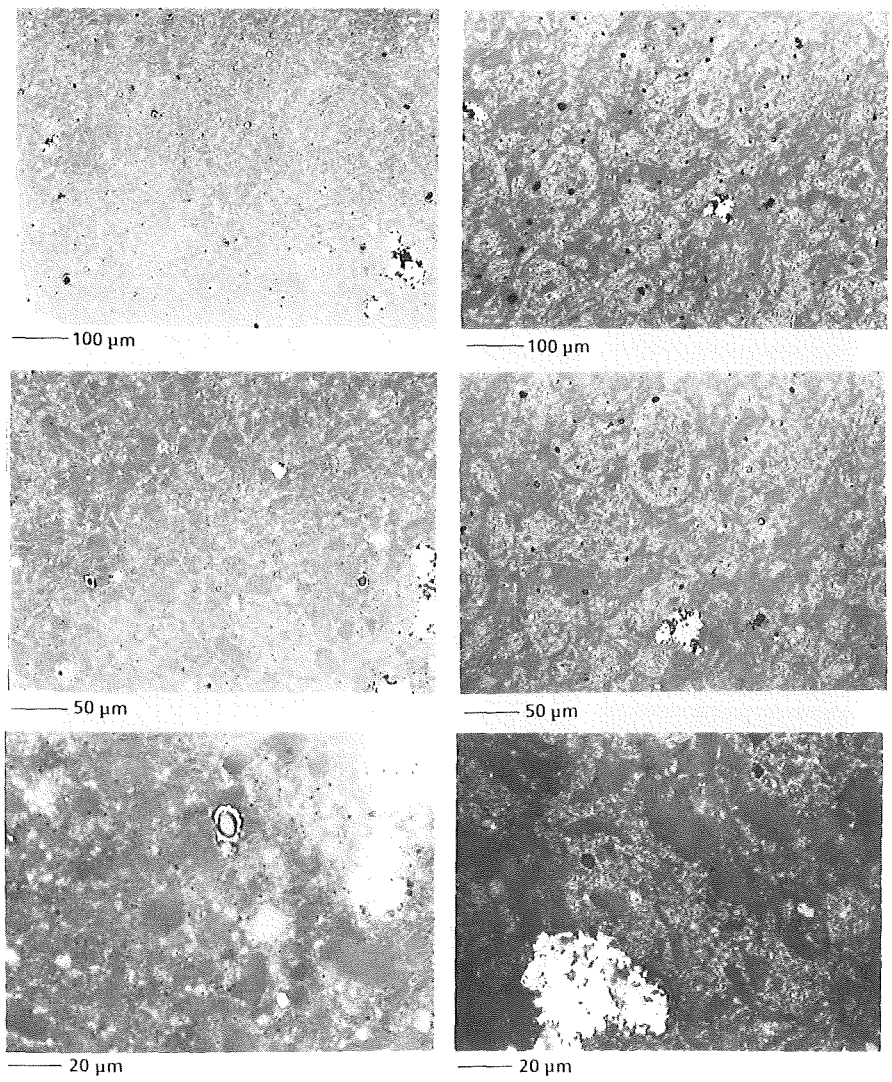

Fig. 15. Micrographs of VG98/12 glass products containing 15 wt% of LWR waste oxides (homogeneous mixture, left) and SG7 glass products containing 15 wt% of SBR waste oxides (inhomogeneous mixture, right) (19 cm diameter).

- Needle shaped crystals which exhibit a structure and a composition similar to the mineral apatite.
- Crystals of a calcium titanium silicate phase of an unknown structure.

The temperature of maximum crystal growth rate was between 920 and 1020 K. The maximum extent of crystallinity after 10 000 h heat treatment at 920 K was

measured between 20 and 30 wt%. At 1020 K this value was reached even after short times, but was not increased by longer treatment.

The crystallization behavior of SG7 glass products was investigated in our own experiments by annealing molten samples up to 28 d at 1020 K. The samples did not contain any waste simulate except ruthenium particles, since these might act as foreign nuclei for crystallization. After 7 d no signs of crystallization could be detected, however after 28 d, two crystalline phases, both dendritic, had formed (cf. fig. 16). The first, taking the shape of a relief from polishing, appears in circular areas and may have grown from heterogeneous nuclei such as Ru particles or pores. The second one, light gray, more flat in appearance, also forms preferentially around heterogeneous nuclei. The concentration of crystals was not sufficient for detection by X-ray diffraction. Obviously, if crystallized areas become larger than about 0.1 mm, stress build-up by volume changes initiates radial micro-cracks around the crystallized areas. However, since the glass products are held only for several hours at such high temperatures during hot-pressing, this crystal formation and micro-cracking will certainly not occur during preparation of the waste form.

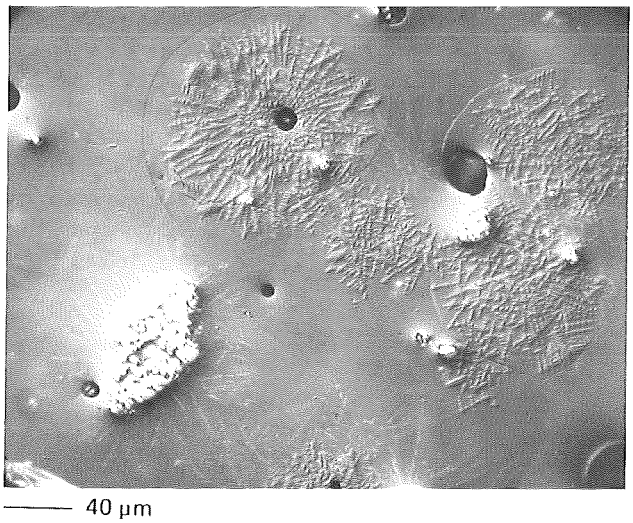

Fig. 16. Beginning crystallization on molten SG7 containing Ru particles, after annealing for 28 d at 1020 K, interference contrast.

The final glass products will be stored for extended times at centerline temperatures, as high as 770 K. Although radiation may also enhance diffusion and crystallization, the higher transition temperature of SG7 (840 K) will probably prevent significant crystallization during long-term storage. In any event, according to literature, it is not expected that chemical durability would be seriously affected by partial crystallization (Wald and Westsik 1979, Chick and Turcotte 1983, Mitamura et al. 1986).

5. Chemical durability

5.1. Glass type and chemical durability

Chemical durability of glass is not much affected by its preparation technique in general. However, because of the higher melting temperatures, glasses developed for melting will usually be a compromise between melting temperature and good chemical durability (which is usually correlated with high melting temperature). By contrast, sintering temperatures are much lower, therefore glasses, more durable than common borosilicate glasses, can be utilized. The newly developed glass SG7 requires hot-pressing temperatures 100 K higher than the borosilicate glass VG98/12, but has at the same time a much enhanced chemical durability.

5.2. MCC-1 tests and soxhlet tests

Chemical durability of VG98/12 and SG7 products was tested according to the MCC-1 procedure at 363 K in doubly distilled water up to 60 d. Most samples were taken from glass blocks of 19 cm diameter, containing 15 wt% of LWR or SBR waste, respectively. To determine the influence of waste loading on chemical durability, also VG98/12 and SG7 samples of 26 mm diameter, containing waste loadings up to 25 wt%, were prepared. The specimens were cut with a low-speed diamond saw to a geometric surface area of 400 mm^2 and subsequently polished to 600 grit. After careful ultrasonic cleaning, samples were tested in teflon containers at a SA/V ratio of 10 m^{-1}. On completion of the test period, weight losses were measured, and the leachants were analyzed by atomic absorption spectroscopy (AAS) or inductive coupled plasma analysis (ICP), respectively. The normalized elemental mass losses (NL_i) were determined according to the formula:

$$NL_i = \frac{m_i}{SA \cdot f_i}, \tag{5.2.1}$$

where

NL_i = normalized elemental mass loss of element i [gm^{-2}],

m_i = detected mass of element i in the leachant [g],

SA = surface area [m^2],

f_i = mass fraction of element i in the unleached specimen.

Time dependence of the mass losses of VG98/12-15LWR (SG7-15SBR) products determined by MCC-1 tests in water at 363 K is depicted in fig. 17 (18).

While boron, silicon, sodium and cesium mass losses of VG98/12 products clearly increase with time, strontium and molybdenum releases of these glasses remain in the same range during the whole testing period of 56 d. In general, the elemental

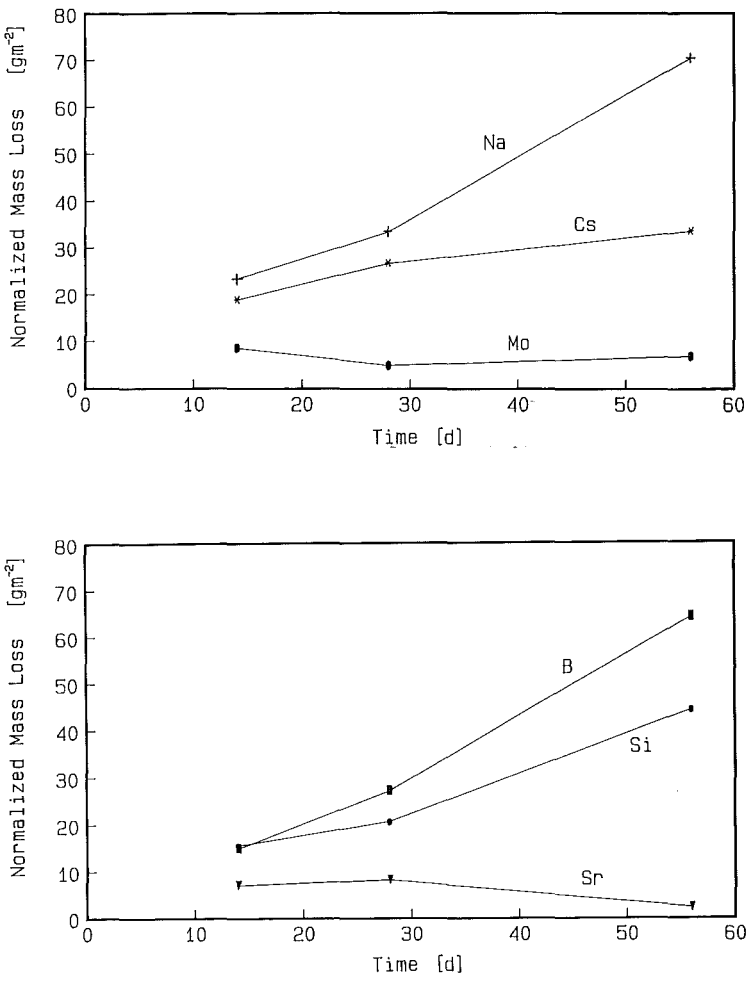

Fig. 17. Normalized mass losses of VG98/12-15LWR, MCC-1, DI water, 363 K.

mass losses of SG7 products are roughly one order of magnitude lower when compared to VG98/12 products. In particular, the main glass network former silicon and also the modifiers sodium and cesium that are normally leached preferentially by ion exchange, exhibit low release rates.

For comparison, MCC-1 tests were also performed on molten borosilicate glass products GP98/12.2 produced in the German LFCM melter. (The samples were supplied by KfK/INE; cf. Weisenburger 1985.) Base glass composition of VG98/12.2 (table 4) is similar to VG98/12. Waste loading was about 13.5 wt%, noble metals included.

In table 5 the results after 28 d corrosion time in water are compared to those obtained with the above hot-pressed glasses. In addition, literature data for the American reference glass PNL76-68 are shown (Pederson et al. 1983). While the

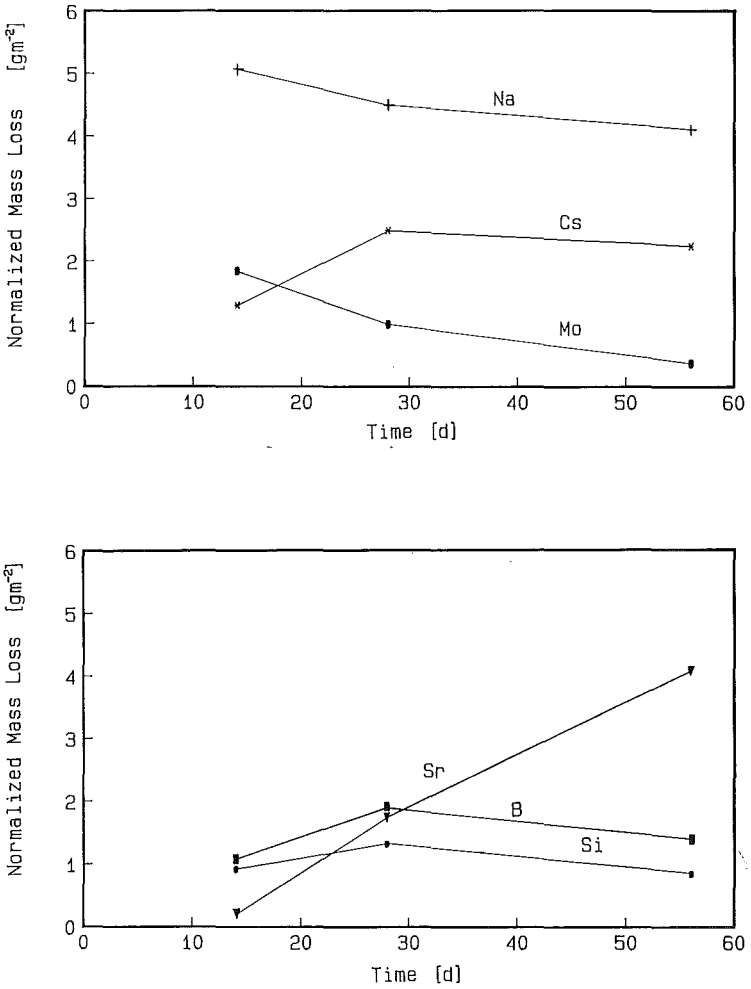

Fig. 18. Normalized mass losses of SG7–15SBR, MCC-1, DI water, 363 K.

molten glasses are in the same range as the hot-pressed VG98/12, the optimized glass SG7 shows a much better performance. This behavior was also confirmed by soxhlet tests on SG7 glass products up to 84 d (fig. 19). Of course, in soxhlet testing corrosion is much more aggressive and faster. But still, the mass losses determined on SG7 glass products by soxhlet testing were slightly lower than the corresponding mass losses determined on VG98/12 glasses by MCC-1 testing.

The influence of waste loading on the corrosion behavior of SG7 products was determined by MCC-1 tests in water for 14 d (fig. 20). Although there might be a minimum at 15 wt% of SBR waste loading, a clear tendency was not determined.

Keeping in mind the network-like distribution of some elements (cf. section 4), the question arises, whether these elements, or the corresponding phases, are

Table 4
Composition of glass frit VG98/12.2 for the German LFCM melter (Weisenburger 1985)

Oxide	wt%
Al_2O_3	2.4
B_2O_3	14.8
CaO	4.5
MgO	2.2
Na_2O	18.6
SiO_2	53.2
TiO_2	4.3

Table 5
Normalized mass losses (MCC-1, DI Water, 363 K, 28 d) of molten glasses PNL76-68 (Pederson et al. 1983) and GP98/12.2 (Weisenburger 1985) and hot-pressed glasses VG98/12-15LWR and SG7-15SBR

	Normalized mass loss [g/m^2]			
Element	PNL76-68	GP98/12.2	VG98/12-15LWR	SG7-15SBR
Si	~17	17.8	19.7	1.3
Na	~25	24.3	28.0	4.5
B	~30	not determined	26.9	1.9
Mo	~31	15.0	5.9	<2
Cs	~32	19.3	21.0	2.5
Sr	not available	8.8	6.6	<3

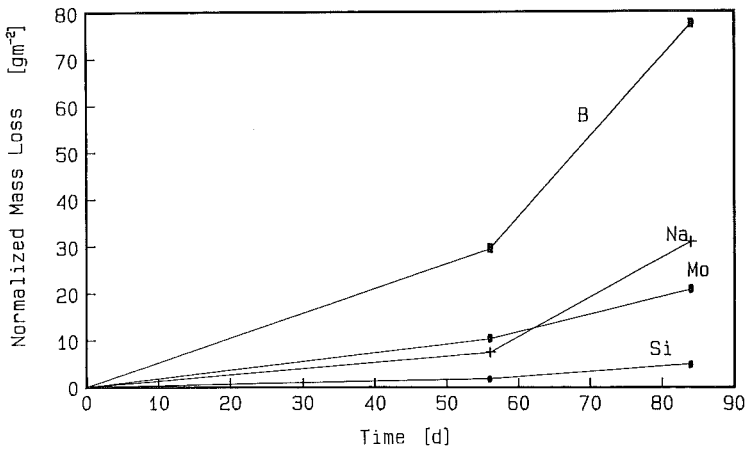

Fig. 19. Normalized soxhlet mass losses of SG7-15SBR.

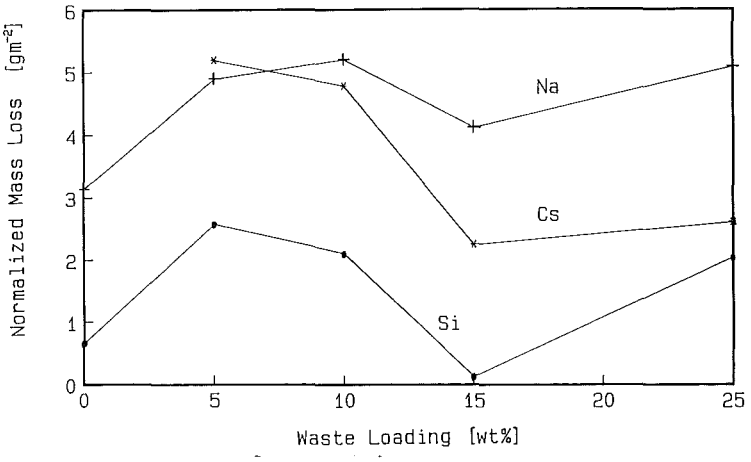

Fig. 20. Influence of waste loading on chemical durability of SG7 with SBR (MCC-1, DI water, 14 d).

interconnected or isolated from each other. Therefore a SG7 glass product containing 15 wt% of SBR waste was leached for 14 d in an autoclave at 473 K under equilibrium pressure. A cross section of the specimen was investigated by energy dispersive X-ray analysis (EDAX). Various elemental distributions are shown in fig. 21 in addition to the secondary electron image visible in the lower right corner. Clearly, sodium, silicon and partially calcium are depleted from the reaction zone that has an average depth of 80 to 100 μm. Most other waste elements still remain captured in the glass matrix, while some of them appear enriched in the reaction zone. Under

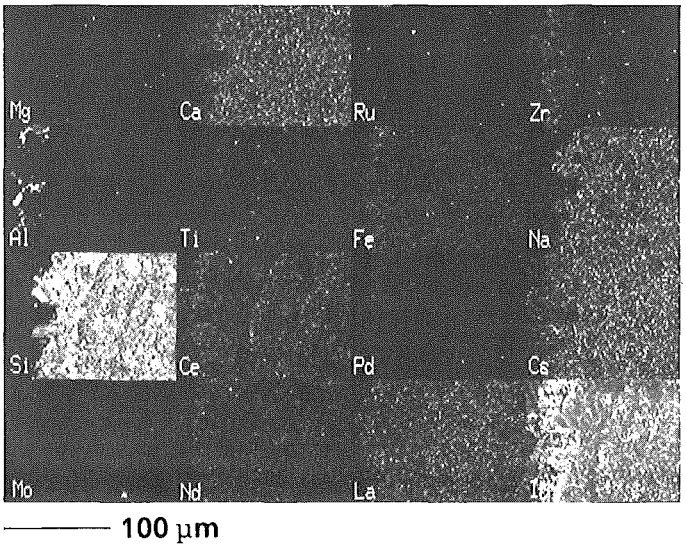

Fig. 21. Cross section of SG7–15SBR product after 14 d of autoclave testing in DI water at 473 K, 1 MPa; secondary electron image (lower right corner) and elemental distributions by EDAX.

these conditions network breakdown of the glass matrix seems to be the main corrosion mechanism, and a preferential attack of waste particles did not occur.

Currently, various MCC-1 tests in quinary salt brine are performed on VG98/12 and SG7 glass products. The analyses have not been completed yet. But primary results indicate that corrosion is much lower in salt brine than in water. Also, the good behavior of SG7 glass products is confirmed. Although further testing is needed, in particular to determine the corrosion mechanism, the above results indicate that chemical durability of hot-pressed glasses can be improved significantly, if more durable base glasses (e.g. higher silicon and aluminum content and lower sodium content) are used.

6. *Physical and mechanical properties*

In general, physical and mechanical properties of VG98/12 and SG7 glass products relevant to final storage (table 6), are similar to borosilicate glass properties. The smaller coefficient of thermal expansion of SG7 glass can be explained by its high silicon and aluminum content and low sodium content.

Table 6
Physical and mechanical properties of hot-pressed VG98/12 (SG7) glass products containing 15 wt% of LWR (SBR) waste simulate

Property	VG98/12-15LWR	SG7-15SBR
Density [kg m^{-3}]	2750±50	2560±50
Coefficient of thermal expansion [a] [10^{-6} K^{-1}]	10.4±0.2	6.8±0.2
Specific heat [Jg^{-1} K^{-1}] at 350 K	0.84±0.02	0.81±0.02
470 K	0.94±0.02	0.92±0.02
670 K	1.08±0.02	1.04±0.02
Thermal conductivity [b] [W m^{-1} K^{-1}] at 350 K	1.05±0.10	1.30±0.10
470 K	1.15±0.10	1.44±0.10
670 K	1.24±0.10	1.60±0.10
Young's modulus [GPa]	73±3	73±3
Poisson's ratio	0.24±0.01	0.22±0.01
Transverse rupture strength [MPa]	35.9±7.6	32.0±7.6

[a] Linear thermal expansion in the range 300-625 K.
[b] Calculated from thermal diffusivity measurements and specific heat data.

Density, Young's modulus, Poisson's ratio, and transverse rupture strength were measured on hot-pressed samples of 19 cm diameter. As can be seen from table 6 and fig. 6, densities of technical size samples and laboratory-scale samples are comparable. Young's modulus and Poisson's ratio were measured using the ultrasonic method (this method may yield slightly higher values for Young's modulus than tensile testing), while transverse rupture strength was tested by four-point bending. Specific heat, thermal diffusivity, and the coefficient of thermal expansion were measured on laboratory-scale samples using calorimetry, the laser flash method,

and differential dilatometry. Thermal conductivity was calculated from thermal diffusivity measurements and specific heat data.

7. Summary and conclusions

Hot-pressed glass is a waste form suitable for the immobilization of high-level waste from the reprocessing of light water reactor and fast breeder fuel. The basic process has been investigated and optimized. After denitration with formaldehyde, the simulated HLW is mixed with glass frit and simultaneously dried in an oil-heated mixer. After "in-can calcination" for at least 24 h at 850 or 950 K (depending on the type of waste and glass), the mixture is hot-pressed for several hours at 920 or 1020 K respectively, at pressures between 0.4 and 1.0 MPa. Subsequent slow cooling avoids fracturing of the product (cooling rate <2 K/h). The final products do not represent homogeneous solid solutions of waste oxides in glass. The waste elements are rather heterogeneously embedded in the glass matrix, some elements however, such as cesium, tend to diffuse into the matrix homogeneously.

The technology has been demonstrated with inactive HLW simulates; products up to diameters of 30 cm were highly dense ($\geq 95\%$ TD) and macroscopically homogeneous. When compared to glass melting, vitrification by powder technology leads to an important reduction in processing temperatures (~ 500 K). The temperature reduction and the absence of the liquid state offers some major advantages:

- The production of secondary waste by evaporation losses is reduced considerably.
- Segregations and macroscopic inhomogeneities, as well as melter corrosion problems are excluded.
- Variations of waste composition and waste loading affect processing conditions and product performance only to a minor extent; waste loadings up to 35 wt% were demonstrated.

In addition, the process is simplified by the use of containers that can be easily arranged and stacked to any chosen height. Although in general physical and mechanical properties of molten and sintered glasses are comparable, chemical durability of hot-pressed glass products is markedly enhanced by the utilization of more durable glasses (e.g. higher silicon and aluminum and lower sodium content).

Because of the potentially lower throughput in batch processing the process is specially suited if higher product quality is desired. Sintered glass technology may even save cost, if smaller waste streams have to be handled, since it does not require expensive adaptation of glass properties to the particular waste stream. Also, even dissolver sludge containing metal cuttings from fuel rods can be immobilized in sintered glass, thus eliminating the need for separate conditioning (cf. Ondracek and Toscano 1984).

The state of process development cannot be compared to borosilicate glass melting technology. All samples, produced so far, were inactive. The adaptation of process technology to hot cell conditions will require considerable future research and development. For remote handling, also the heatable mixer may have to be modified.

A heatable drum dryer, developed and tested in hot cells by Halaszovich (1979) may replace the heatable mixer. Likewise a sol-gel process (cf. Lackey et al. 1980, Cecille 1981), usually leading to intimate mixtures and fine powders that are easily sintered, might offer a good alternative to the mixing step.

Investigation of chemical durability will need further testing, in particular with radioactive products. The application of surface analytical techniques, such as SEM, EDAX, SIMS and electron microprobe analysis, will also help determine the corrosion mechanism. In addition, further work is needed to identify the phases formed during hot-pressing. But in general, because of the predominantly heterogeneous embedding of waste, product properties should not be as sensitive to phase formation and changes over time, as the properties of glasses prepared by melting.

Acknowledgments

The authors wish to express particular thanks to Mr. K. Spieler, who did great work in developing the technical equipment. Dr. C. Adelhelm and her group performed the analytical work and gave helpful advice with corrosion testing. Dr. M.A. Audero reviewed the manuscript and gave several comments. Mrs. Haase carefully measured physical and mechanical properties. Some of the specific heat data were determined at IRE Stuttgart. All these contributions are gratefully appreciated by the authors.

References

Bauer, C., and G. Ondracek, 1983, Atomkernenerg. Kerntech. **43**, 55.

Bevilacqua, A.M., D.O. Russo, N. Messi de Bernasconi and M.A. Audero, 1985, Proc. Conf. Asociacion Argentina de Technologia Nuclear.

Cecille, L., 1981, IAEA-SM-**246**/22.

Chick, L.A., and R.P. Turcotte, 1983, PNL-**4576**.

Cutler, I.B., and R.E. Henrichsen, 1968, J. Am. Ceram. Soc. **51**, 604.

Frenkel, J., 1945, J. Phys. **9**, 385.

Guber, W., M. Hussain, L. Kahl, G. Ondracek, J. Saidl and Th. Dippel, 1979, Report No. KfK-2721 (Kernforschungszentrum Karlsruhe).

Halaszovich, S., 1979, Verfestigung hochradioaktiver Spaltproduktlösungen aus der Wiederaufarbeitung abgebrannter Brennelemente für eine Endlagerung, Dissertation TH Aachen.

Kingery, W.D., and M. Berg, 1955, J. Appl. Phys. **26**, 1205.

Kuczynski, G.C., 1949, J. Appl. Phys. **20**, 1160.

Lackey, W.J., R.E. Blanco and A.L. Lotts, 1980, Nucl. Technol. **49**, 321.

Macedo, P.B., D.C. Tran, J.H. Simmons, M. Saleh, A. Barkatt, C.J. Simmons, N. Lagakos and E. DeWitt, 1979, Porous glass matrix method for encapsulating high-level nuclear wastes, in: Proc. Conf. on Ceramics in Nuclear Waste Management, Cincinnati, OH, 1979, eds T.D. Chikalla and J.E. Mendel (Technical Information Center, DOE) p. 321.

Macedo, P.B., A. Barkatt and J.H. Simmons, 1982, A flow model for the kinetics of dissolution of nuclear waste forms: A comparison of borosilicate glass, Synroc and high-silica glass, in: Proc. Conf. on Scientific Basis for Nuclear Waste Management V, Berlin, 1982, ed. W. Lutze (North-Holland, Amsterdam) p. 57.

Meyer, K., 1968, Physikalisch-chemische Kristallographie (VEB Deutscher Verlag der Wissenschaften, Berlin) pp. 296–297.
Mitamura, H., T. Banba and T. Murakami, 1986, Nucl. & Chem. Waste Manage. **6**, 223.
Ondracek, G., and E.H. Toscano, 1984, J. Nucl. Mater. **124**, 75.
Pederson, L.R., C.Q. Buckwalter and G.L. McVay, 1983, Nucl. Technol. **62**, 151.
Ross, W.A., 1975, Report No. BNWL-SA-5362 (Battelle Pacific Northwest Laboratories).
Scholze, H., 1966, Glass Ind. **47**, 546; 622; 670.
Skokan, A., and V. Schauer, 1982, Microstructures and crystallization in simulated waste glasses, in: Proc. Treatment and Handling of Radioactive Wastes, Hanford, 1982, eds A.G. Blasewitz, J.M. Davis and M.R. Smith (Batelle Press, Columbus, Richland; Springer, Berlin).
Terai, R., M. Kinoshita and K. Eguchi, 1978, Osaka Kogyo Gijutsu Shikenjo Kiho **29**, 36.
Thümmler, F., 1963, Wissenschaftliche Grundlagen der Sintervorgänge, in: Fortschritte der Pulvermetallurgie, Bd. 1, ed. F. Eisenkolb (Akademie-Verlag, Berlin) ch. 5.
Wald, J.W., and J.H. Westsik, 1979, Devitrification and leaching effects in HLW glass – comparison of simulated and fully radioactive waste glass, in: Proc. Conf. Ceramics in Nuclear Waste Management, Cincinnati, OH, 1979, eds T.D. Chikalla and J.E. Mendel (Technical Information Center, DOE) p. 277.
Weisenburger, S., 1985, in: Report No. KfK-3886 (Kernforschungszentrum Karlsruhe).